

NONLINEAR CRASH DYNAMICS SIMULATION OF NOVEL AIRBAG BASED NEXT GENERATION ENERGY ABSORBING BARRIER

Rahul Gupta and Ajit D. Kelkar
Computational Science and Engineering
North Carolina A & T State University,
Greensboro, NC 27411
Tel. (336)-334-7620 x324
Fax: (336)-334-7417
Email: rgupta@ncat.edu

ABSTRACT

The fatality analysis report system of the National Highway Traffic Safety Administration reported that around 42,000 people in United State are still being killed annually in motor vehicle crashes. Approximately 30 percentage of the fatality are from crashes involving in collisions with roadside objects. Energy absorbing barriers (EAB) such as concrete median barriers, guardrails and other forms of impact attenuators are designed to absorb and dissipate the kinetic energy of run-off-the road vehicles efficiently. The main roles of the EAB are to increase vehicle occupant survivability and reduce injury levels by smoothly redirecting an errant vehicle to bring it a controlled stop. Non-linear, three-dimensional, finite element code LSDYNA-3D is used to perform realistic and predictive virtual crash simulations for analyzing the large-deformation dynamic responses of elastic or inelastic structures using explicit time integration schemes.

This paper presents a novel airbag technology, fluid-structure interaction effect based patented EAB designed and tested by the researchers at NC A&T State University primarily for high velocity impacts. Simulation and testing of the new EAB has shown marked improvement compared to the current generation of EAB. The analysis consists of crash deformation profile, acceleration records at different locations, and energy absorptions by different components.

INTRODUCTION

Statistics shows that an injury occurs every 9 seconds and a death occurs every 13 minutes in the USA as a result of car accidents. Full frontal impact crashes are the most severe in terms of injuries and deaths on the road, as they represent one fourth of all frontal collisions. A vehicle crash at 40 mph can cause 100G in 100 milli seconds. To place things in perspective, an astronaut in a spacecraft experiences 3G at takeoff and pilots in aircraft tend to pass out at 6G. Thus, the effect of 100G on car drivers can be extremely serious.

GM performed early vehicle testing in 1924. This type of testing was focused primarily on the vehicle structure. Between the years 1920-1964, auto fatality rates

doubled and in 1966 auto safety laws were enacted. In 1971, airbag crash tests were performed with human subjects. These were the earliest efforts in safety testing.

Today, agencies such as the National Highway Traffic Safety Administration (NHTSA), the Insurance Institute for Highway Safety (IIHS), the US Department of Transportation, and the National Crash Analysis Center (NCAC), among others, are responsible for testing vehicles to ensure that there is a reduction of deaths, injuries, and economic loss resulting from motor vehicle accidents. Setting and enforcing safety performance standards for all motor vehicles is accomplished in this manner. Testing by these agencies is similar. The USDOT tests cars by colliding them head-on into a flat wall at 35 mph and evaluating their performance in serious frontal crashes. The IIHS performs off-center crash tests at 40 mph that create circumstances similar to those involved in a frontal offset crash between two vehicles of the same weight. After performing these crash tests, engineers examine the car to see if it maintains a reasonable amount of survival space so that passengers may walk away from an accident. The engineers also examine the crush zone of the car to see if it absorbs the majority of the energy from the collision.

Through this approach, researchers and engineers investigate, analyze and quantify the roles and performance of vehicles, occupants and roadside hardware in crashes, both individually and in combination. They conduct statistical analyses of crash data; undertake hospital studies to relate crash events to occupant injuries; incorporate state-of-the-art investigation methods and biomechanics research to determine injury patterns; and evaluate vehicle and roadside hardware crash performance by reviewing crash test films and crash data with the use of cutting-edge computer modeling.

COMPUTER SIMULATION USING FINITE ELEMENT MODELING

Computer simulation for vehicle crashworthiness evaluation has contributed greatly to shortening the development periods for new vehicles with its advantages in numerical simulation techniques and computational capabilities. The main purpose of crashworthiness simulations is to evaluate structural performance and occupant injury criteria under various crash scenarios in the early stages of the design process.

Finite element analysis (FEA) is an extremely efficient and cost-effective tool to assist in the design of safer highway guardrails, bridge supports, signposts, and other roadside structures. FEA, which can be used to predict the outcome of a crash test, provides the potential to prevent some of the 500,000 human injuries and 13,000 premature deaths resulting from motor vehicles that run-off-the-road and either rollover or are involved in collisions with a roadside object or feature.

Traditional methods of designing roadside structures, by crashing vehicles into them, are extremely costly—more than \$25,000 per crash—and they do not always provide definitive information. FEA can reduce the cost and time to develop roadside safety structures by replacing the trial and error process of crash testing with computer crash analysis. Using FEA can reveal, with much greater insight, what actually happens and what effect a design change may have.

RIGID BARRIER RESEARCH

Researching rigid roadside barriers (under the appropriate test conditions specified in NCHRP Report 350) on the effects of higher speed limits on impact speed and the appropriateness of 25 degrees for the impact angle, Bligh [1] suggested i) to maintain the current test impact speed of 100 km/h (62.2 mph), ii] to maintain the current impact angle of 25 degrees for test 11 of the length-of-need sections of permanent longitudinal barriers, iii] to reduce the test impact angle from 25 to 20 degrees for test 11 of the length-of-need sections of the temporary longitudinal barriers, iv] to reduce the test impact angle from 25 to 20 degrees for test 21 of the barrier transition sections.

Consalzio et al [2,3] proposed a new low profile portable concrete barrier system that was developed for use in roadside work zone environments. It was shown that the extensive use of nonlinear dynamic finite element simulation could accomplish several cycles of conceptual design refinement without expensive full scale crash testing.

FLEXIBLE ALTERNATE MATERIAL BARRIER RESEARCH

Botkin et al [4] coordinated with Lawrence Livermore National Laboratory, Oak Ridge National Laboratory, Sandia National Laboratory, Argonne National Laboratory, and Los Alamos National Laboratory to work in three distinctly different technical areas, one of which was composites material modeling for crashworthiness with the primary use of LSDYNA-3D. An excellent agreement has been found between tube crush simulations and the experiments.

Reid, Sicking et al [5] worked on SAFER Barrier developments. For many years, containment for errant racing vehicles traveling on oval speedways has been provided through the use of rigid, concrete containment walls placed around the exterior of the tracks. However, accident experience has shown that serious injuries, and even fatalities, may occur as a result of vehicular impacts into these non-deformable barriers. Because of these injuries, the Midwest Roadside Safety Facility at the University of Nebraska-Lincoln was sponsored by the Indy Racing League and the Indianapolis Motor Speedway, and later joined by NASCAR, to develop a new barrier system that could improve the safety of drivers participating in auto racing events. Over the course of the project, several barrier prototypes were investigated and evaluated using static and dynamic component testing, LS-DYNA computer simulation modeling, and a total of 20 full-scale vehicle crash tests. The full-scale crash-testing program included bogie vehicles, small cars, a full-size sedan, as well as actual IRL open-wheeled cars and NASCAR Winston Cup cars. For the racecar impact tests, typical impact speeds and angles ranged approximately from 190 to 245 km/h (120 to 150 mph) and 20 to 25.6 degrees, respectively. During this research effort, a combination steel tube skin and foam energy-absorbing barrier system, referred to as the SAFER barrier, was successfully developed. Subsequently, the SAFER barrier was installed at the Indianapolis Motor Speedway in advance of the running of the 2002 Indy 500 mile race. From the results of the laboratory-testing program as well as from the accidents occurring with the SAFER barrier during practice, qualifying, and the race, the SAFER barrier was shown to provide improved safety for drivers impacting the outer walls.

FINITE ELEMENT METHOD IN CRASHWORTHINESS RESEARCH

Jiang et al [6] presented equations for determining the peak impact load of a car crashing into a rigid concrete safety barrier. The equations were validated using full-scale crash tests performed by different research institutions, including Monash University. Comparisons between theory and test results indicated that the equations provided reasonable accuracy when predicting peak impact loads of a car crashing into a rigid concrete barrier for different impact speeds and angles. In particular, these equations could provide bridge engineers a useful means to determine realistic peak impact service loads for designing bridge deck barriers.

Karma et al [7] evaluated rigid concrete barriers using LSDYNA-3D. Dynamic non-linear finite element methods were extensively used to analyze vehicle-to-barrier crashes. The underlying challenge in this analysis was the capability of the constitutive models of concrete to represent a realistic response of the barrier under impact loading. LS-DYNA, a commercial FE code for crashworthiness analysis, offered four major constitutive models for concrete. The performance of each of these models was assessed by comparisons among numerical simulations and benchmark stress-strain data that were obtained from triaxial experiments conducted on plain concrete.

Kelkar et al [8] researched Simulation of the Ford Taurus Frontal Offset Impact on the EEVC Fixed Deformable Barrier.

Kirkpatrick et al [9] worked on the Development of an LS-DYNA Occupant Model for use in Crash Analyses of Roadside Safety Features. Using the correct combination of deformable and rigid components resulted in an occupant model that was computationally efficient and capable of simulating occupant kinematics in a collision.

Mackerle [10] provided bibliographical review of finite element analyses and simulations of crashes and impact-induced injuries from the theoretical as well as the practical point of view.

Ray et al [11] assessed how well a finite element analysis of a collision event simulated a corresponding full-scale crash test. The method was used to compare a series of six identical crash tests and was also used to compare a finite element analysis to a full-scale crash test.

Wekezer [12] presented the research results of a study, in which computational mechanics was used to predict vehicle trajectories traversing standard Florida DOT street curbs. Computational analysis was performed using LS-DYNA non-linear, finite element computer code with two public domain, finite element models of motor vehicles: the Ford Festiva and the Ford Taurus. Shock absorbers were modeled using discrete spring and damper elements. Connections for the modified suspension systems were carefully designed to assure a proper range of motion for the suspension models. Inertia properties of the actual vehicles were collected using tilt-table tests and were used for LS-DYNA vehicle models. Full-scale trajectory tests were performed at Texas Transportation

Institute to validate the numerical models and the predictions from computational mechanics. Experiments were conducted for the Ford Festiva and the Ford Taurus, both for two values of the approach angle: 15 and 90 degrees with an impact velocity of 45 mph. Experimental data including accelerations, displacements and overall vehicles behavior were collected by high-speed video cameras and were compared with numerical results. Verification results indicated a good correlation between computational analyses and the full-scale test data. The study also underlined a strong dependence of properly modeled suspension and tires on resulting vehicle trajectories.

MOTIVATION FOR FLEXIBLE EAB RESEARCH

Large amounts of kinetic energy must be dissipated when a moving vehicle impacts a relatively immovable object like a barrier. Speed is important because it is multiplied by itself and the weight of the vehicle to calculate the kinetic energy that must be overcome. ($KE = \frac{1}{2} MV^2$).

This resistance of the barrier is the result of the strength to resist the impact multiplied by the duration of the impact. For example, a pile of hay can slow a speeding vehicle to a stop over time, as a massive concrete wall instantaneously does. In this manner, designs that create a progressive impact by virtue of their three dimensional shapes are more effective due to their mass than they are for a conventional flat concrete wall.

A moving vehicle has kinetic energy. The faster it moves, the more kinetic energy it has. The kinetic energy of a moving vehicle is proportional to the square of the velocity; therefore, a car traveling at 50 mph has four times the kinetic energy of the same car traveling at 25 mph.

A crash barrier works by removing the kinetic energy of the moving vehicle. It may accomplish this removal in several ways:

1. **RIGID BARRIER:** By being very rigid and strong, which keeps the vehicle from traveling further. This kind of crash barrier is very rigid and it cannot move much, so it does not absorb much energy. The vehicle has to absorb its own kinetic energy by deforming. If the vehicle itself is very strong and rigid, the impact forces can be extremely large.
2. **SOFT IMPACT BARRIER:** By soaking up the kinetic energy, like a sponge. This means that the crash barrier does not need to be as strong and rigid as it stops the vehicle by a plowing action. In many cases, the vehicle will be almost unharmed, as the barrier itself does the work. A correctly designed energy absorbing crash barrier must be relatively weak, as it needs to deform readily. This keeps the reaction forces relatively low.

Under explosive conditions or crash conditions, an energy-absorbing barrier is always better than a rigid barrier. This has been proven by many tests. Rigid barriers

will fail under relatively small impact velocities, while energy-absorbing barriers will be able to survive much higher velocities.

Another difference in these barriers lies in the way in which the barriers absorb energy. The energy absorbed is roughly the reaction force multiplied by the distance that the barrier travels as it stops the vehicle, so the more distance the barrier travels through, the lower the force.

A rigid retaining wall does not travel very far when it stops a vehicle, only an inch or so at the most. Therefore, the force on the barrier is very large. An energy-absorbing barrier (EAB), on the other hand, stops the vehicle through a stroke of several inches. Therefore, the stopping forces are relatively low.

A majority of the current research work has been in the area of Rigid Barrier development. A minority of the current research work has been in the area of Flexible Barrier development. Major thrusts have been made in the development of cost effective solutions, thereby compromising safety criteria.

Reid, Sicking et al [5] investigated SAFER Barrier development. During their research, a combination steel tube skin and Polystyrene energy-absorbing barrier system was developed. Its purpose was to cushion the effects of force through energy absorption and distribution. Bundles of extruded, closed cell polystyrene were placed between the rigid concrete barrier wall and the steel tubes every ten feet. However, the SAFER barrier is not really a flexible barrier and deforms very little as compared to the Airbag EAB.

The goal of this research is to develop an optimum cost effective novel technology based EAB geared towards safety and security of the vehicle and its occupants. A correctly designed EAB must be relatively weak, as it needs to deform readily to keep reaction forces low.

ANALYTICAL FORMULATION OF AIR-DAMPENED FLEXIBLE EAB

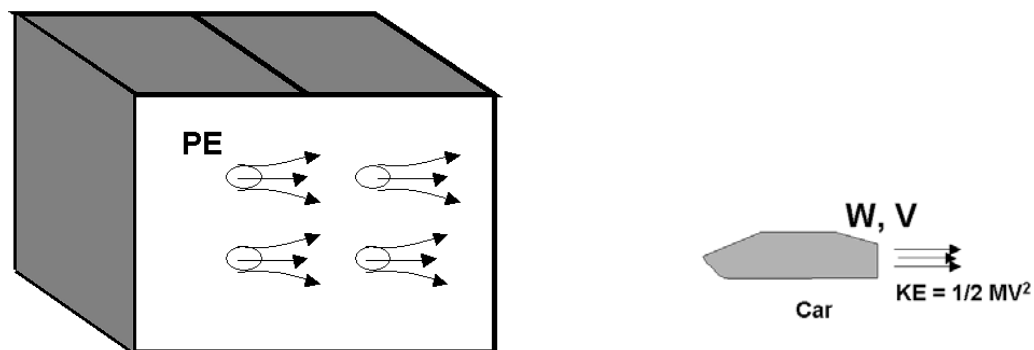


Figure 1. Air-Dampened Flexible Barrier

Figure 1 and 2 shows the energy transfer mechanism, which depends on:

Flexibility & Size of the barrier
Diameter & Number of the holes
Density of the fluid/air
Car speed and mass

(Assumptions: Wall is highly flexible and instantaneous energy transfer occurs)

ENERGY TRANSFER ANALYTICAL EQUATIONS

$$(KE)_{\text{Impact}} \Rightarrow (PE)_{\text{Fluid/Air}} \Rightarrow (PE)_{\text{Fluid/Air}} \text{ Decreases as the air is expelled}$$

$$(PE)_{\text{Fluid/Air}} @ t = (PE)_{\text{Initial}} - (KE)_{\text{lost by the expelling air}}$$

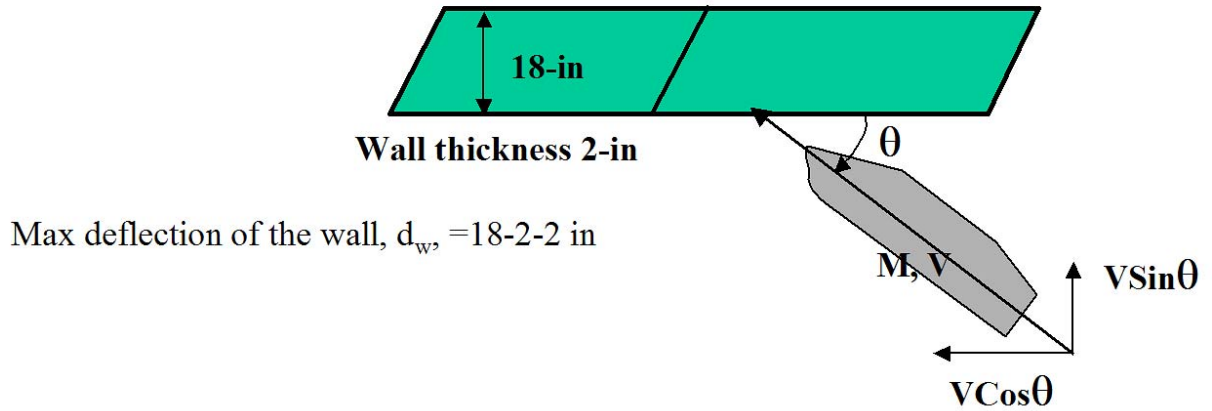


Figure 2. Analytical Model of Air-Dampened Flexible Barrier

Design Parameters

- Max Wt of the car = 4000 lb
- Max Velocity = 153 m/hr
- $g = 32 \text{ ft/Sec}^2$
- Max deflection of the wall, d_w , 14-in

Max deformation of the car, d_c , 4-in

$d_c = 0$ for Rigid car
 $d_c \neq 0$ for non Rigid car

Car deformation

- 4 #s of 2" dia & 0.09' thick
- Length = 5ft
- Axial stiffness $K_a = (4AE/L) = 1.3 \text{ mlb}$

- Transverse stiffness component, $K_c = K_a \sin^2 \theta$
- Anticipated impact force about 300 - 600 kips
- Car frame deflection about 1.5" - 3", other deformations 1" - 2.5"
- Estimated maximum deflection about 4"

Figure 3 shows the “impact force versus impact angle” plots based on the analytical formulation for 4000 lb weight car.

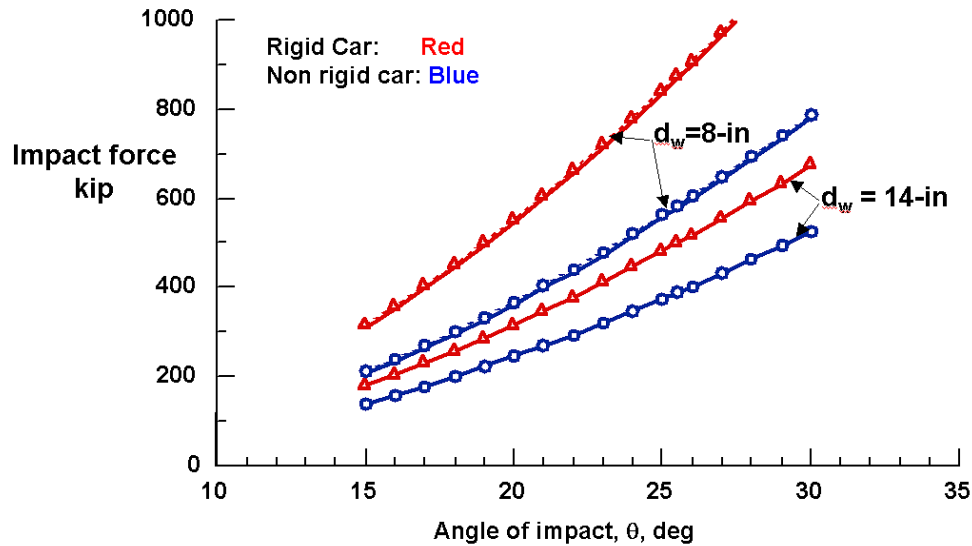


Figure 3. Impact force versus impact angle (car weight 4000 lb)

IMPULSIVE LOADING

When a sudden force strikes a structure, stresses up to twice as large as the values obtained for the same load applied statically may be reached. Shock waves (i.e., stress and strain waves) travel through the structure and may be reflected back from a boundary to the point of the application of the load. Superposition of these waves may result in a doubling up of the stresses where the two waves positively reinforce each other.

HORIZONTALLY MOVING BODY

When weight **W** is in horizontal motion with a velocity **v** arrested by an elastic body the maximum dynamic load is found to be

$$P_{\text{dyn}} / W = \delta_{\text{max}} / \delta_{\text{st}} = K = \sqrt{\frac{v^2}{g \delta_{\text{st}}}} \quad (1)$$

δ_{st} is the static deflection caused by the horizontal force **W**.

QUASI STATIC FINITE ELEMENT ANALYSIS

MATERIAL PROPERTY

The materials used are:

- 1] UHMW HDPE : Ultra High Molecular Weight High Density Polyethylene
- 2] SCANDURA Laminated Rubber

The material properties of the components were determined experimentally. Figures 4 and 5 show the airbag EAB test model and the samples. Table 1 displays the experimentally determined material properties of rubber and UHMW.



Figure 4. Airbag EAB test model




| TESTING OF SCANDURA SAMPLES FOR MODULUS OF ELASTICITY, POISSON'S RATIO AND ULTIMATE STRENGTH | | | | | | | | |
|----------------------------------------------------------------------------------------------|----------|-----------|-------------------------------------------------------------------------------------|----------|-----------|---------------------------------------------------------------------------------------|----------|-----------|
| RAYALON 3-600 MATCHLESS 3/8" X 3/32" | | | USFLEX 440 GIANT 1/4" X 1/8" | | | USFLEX 116600 MATCHLESS 3/8" X 3/32" | | |
| 3-600A | WIDTH | THICKNESS | 440 A | WIDTH | THICKNESS | 11660A | WIDTH | THICKNESS |
| | 0.996 | 0.673 | | 1.092 | 0.593 | | 0.995 | 0.724 |
| | 1.003 | 0.673 | | 1.096 | 0.59 | | 1.046 | 0.727 |
| | 1.005 | 0.667 | | 1.049 | 0.585 | | 1.074 | 0.736 |
| AVERAGE | 1.001 | 0.671 | AVERAGE | 1.079 | 0.589 | AVERAGE | 1.038 | 0.729 |
| AREA | 0.671671 | | AREA | 0.635531 | | AREA | 0.756702 | |
| 3-600B | | | 440 B | | | 11660B | | |
| | 1.024 | 0.676 | | 1.044 | 0.585 | | 1.132 | 0.722 |
| | 1.022 | 0.673 | | 0.995 | 0.59 | | 1.137 | 0.728 |
| | 1.017 | 0.666 | | 1.001 | 0.593 | | 1.125 | 0.735 |
| AVERAGE | 1.021 | 0.6672 | AVERAGE | 1.013 | 0.589 | AVERAGE | 1.131 | 0.728 |
| AREA | 0.668011 | | AREA | 0.596657 | | AREA | 0.817304 | |
| ALL VALUES ARE IN INCHES | | | | | | | | |
|  | | |  | | |  | | |
| 3-600 | | | 440 | | | 11660 | | |

Figure 5. Material property after testing

Table 1. Material property testing result

| Material | Modulus E psi | Poisson's Ratio | Ultimate Tensile Strength psi |
|--------------------|--------------------------|----------------------------|----------------------------------------------|
| UHMW - HDPE | 145000 | 0.35 | 6820 |
| SCANDURA 1 | 12000 | 0.04 | 2736 |
| SCANDURA 2 | 10000 | 0.03 | 2457 |
| SCANDURA 3 | 10330 | 0.035 | 1740 |

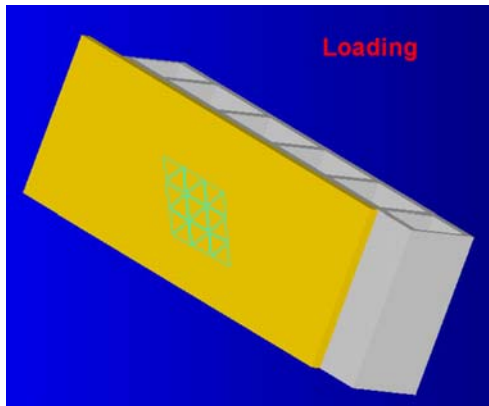


Figure 6. Patch pressure load for airbag EAB

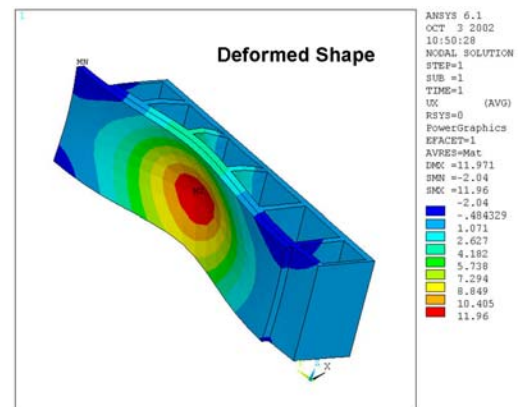


Figure 7. Axial displacement plot of airbag EAB

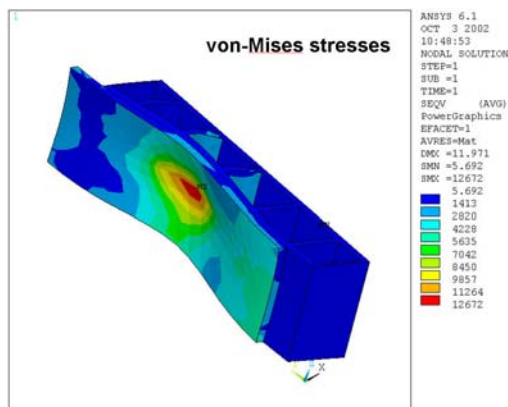


Figure 8. VMS plot of airbag EAB

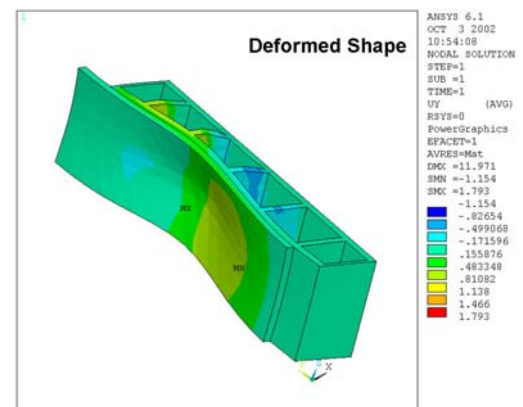


Figure 9. Shear displacement plot of airbag EAB

FEA Software used: ANSYS
Degrees of freedom: 3 translational
Simulated Impact Force: 672 kips

Figure 6 shows the patch pressure loading applied to simulate the bumper impact. Figures 7-9 show the Von Mises stress and the displacement plots.

NON-LINEAR LSDYNA-3D ANALYSIS (AIRBAG EFFECT)

LSDYNA-3D impact simulation is performed on an EAB. The dynamic simulation parameters and results are explained below, and are accompanied by plots.

A rigid car body of 4000 lb weight hits the barrier wall at 90 MPH velocity (car modeled through rigid structure). Simulation is held for 20 ms (0.02 sec). The rib angle is 0 degrees, the car hits at a 25.5° angle. The EAB is wrapped with a 1/8" rubber skin. Tied-Surface-To-Surface contact elements are applied between the front wall and the rubber part and between the rubber skin and the front wall and the rubber part. Automatic surface-to-surface contact elements are applied between the bumper and the front wall and the rubber skin. Airbag control volume with Airbag *MAT_FABRIC properties are applied for the airbags. Automatic surface-to-surface elements are applied between the airbags and the chambers. Automatic single-surface contact is applied inside the airbags.

The back of the rubber wall is fixed. A symmetric Boundary condition has been used at the side edges to simulate a continuous barrier wall. Each unit of the barrier is 96 inches long, 18 inches in depth, and 40 inches in height. Two identical units were laid side by side for the impact simulation (Figure 11).

The plots on the following pages display LSDYNA-3D based nonlinear dynamic finite element simulation for both the non-Airbag EAB as well as Airbag EAB and present the comparative results summary at the end.

LSDYNA 3D AIRBAG CONTROL VOLUME MODELING

A direct approach for modeling the contents of the airbag is to discretize the interior of the airbag with the use of solid elements. The total volume and pressure-volume relationship of the airbag is then a sum of all the elemental contributions. Although the direct approach method may be applied in a straightforward manner to an inflated airbag, it is very difficult to implement during the inflation phase of an airbag deployment. In addition, as the model is refined the solid elements quickly overwhelm all of the other computational costs and make the airbag numerical simulations prohibitively expensive.

An alternate approach for calculating the airbag volume that is both applicable during the inflation phase and less computationally demanding treats the airbag as a control volume. The control volume is defined as the volume enclosed by a surface. In

the present case, the control surface that defines the control volume is the surface modeled by the shell or membrane elements that comprise the airbag fabric material.

Because the evolution of the control surface is known, (the position, orientation, and current surface area of the airbag fabric elements are computed and stored at each time step), these properties of the control surface elements can be used to calculate the control volume, (i.e. the airbag volume). The area of the control surface can be related to the control volume through Green's Theorem

$$\iiint \phi (\partial \psi / \partial x) dx dy dz = - \iiint \psi (\partial \phi / \partial x) dx dy dz + \int_s \phi \psi n_x d\Gamma \quad (2)$$

where the first two integrals are integrals over a closed volume, (i.e. $dv = dx dy dz$), the last integral is an integral over the surface that encloses the volume, and n_x is the direction cosine between the surface normal and the x direction (corresponding to the x-partial derivative); similar forms can be written for the other two directions. The two arbitrary functions ϕ and ψ need to be integrated only over the volume and the surface.

The integral form of the volume may be written as

$$V = \iiint dx dy dz \quad (3)$$

Comparing the first of the volume integrals in Eqn (2) to Eqn (3) the volume integral from Eqn (3) may be easily obtained by choosing two arbitrary functions

$$\phi = 1 \quad (4)$$

$$\psi = x \quad (5)$$

$$\text{leading to } V = \iiint dx dy dz = \int_s x n_x d\Gamma \quad (6)$$

The surface integral in Eqn (6) can be approximated by summation over all the elements comprising the airbag,

$$\int_s x n_x d\Gamma = (\sum x_i n_{ix} A_i), i=1,N \quad (7)$$

for each element i , x_i is the average x coordinate, n_{ix} is the direction cosine between the elements normal and the x direction, and A_i is the surface area of the element.

LSDYNA-3D FABRIC MATERIAL MODEL FOR AIRBAG

The LSDYNA fabric model is a variation on the Layered Orthotropic Composite material model (Material 22) and is valid for only 3 and 4 node membrane elements. This material model is strongly recommended for use in airbags and seatbelts. In addition to being a constitutive model, this model also invokes a special membrane element formulation that is better suited to the large deformations experienced by fabrics. For thin fabrics, buckling (wrinkling) can occur with the associated inability of the structure to

support compressive stresses; a material parameter flag is included for this option. A linear elastic liner is also included which can be used to reduce the tendency for these material / elements to be crushed when the no-compression option is invoked.

If the airbag material is to be approximated as an isotropic elastic material, then only one Young's modulus and Poisson's ratio should be defined. The elastic approximation is very efficient because the local transformations to the material coordinate system may be skipped. If orthotropic constants are defined, it is very important to consider the orientation of the local material system and use great care in setting up the finite element mesh.

EQUATION OF STATE MODEL

At each time step in the calculation, the current volume of the airbag is determined from the control volume calculation. The pressure in the airbag corresponding to the control volume is determined from an equation of state (EOS) that relates the pressure to the current gas density (volume) and the specific internal energy of the gas.

The EOS for the airbag simulations is the usual "Gamma Law Gas Equation of State".

$$P = (k - 1) \rho e \quad (8)$$

where p is the pressure, k is a constant defined below, ρ is the density, and e is the specific internal energy of the gas. The derivation of the EOS is from thermodynamic considerations of the adiabatic expansion of an ideal gas. The change in internal energy dU in n moles of an ideal gas due to an incremental increase in temperature dT , at constant volume is given by

$$dU = n c_v dT \quad (9)$$

where c_v is the specific heat at constant volume. Using the ideal gas law dT may be related to dP and dV as

$$d(pv) = nRdT \quad (10)$$

where R is the universal gas constant. Solving Eqn (10) for dT and using Eqn (9)

$$dU = c_v d(pv)/R = d(pv)/(k-1) \quad (11)$$

$$R = c_p - c_v \text{ and } k = c_p/c_v$$

Eqn (11) may be written as

$$dU = [\rho_0 v_0 / (k-1)] d(p/\rho) \quad (12)$$

and integrated to yield

$$e = (U / \rho_0 v_0) = p / \rho(k-1) \quad (13)$$

Solving for pressure,

$$P = (k-1) \rho e \quad (14)$$

The EOS and control volume calculation may only be used to determine the pressure when the specific internal energy is also known. The evolution equation for the internal energy is obtained by assuming

$$dU = -pdV \quad (15)$$

The minus sign is assigned since dV is negative when the gas is compressed. The expression may be written in terms of the specific internal energy as

$$de = [dU / \rho_0 v_0] = [-pdv / \rho_0 v] \quad (16)$$

$$de / e = (k-1) \rho dv / \rho_0 v_0 = - (k-1) dv / v \quad (17)$$

integrating (17),

$$\ln e = (1-k) \ln V, \text{ i.e. } e_2 = e_1 [v_2/v_1]^{(1-k)} \quad (18)$$

The specific internal energy evolution equation, Eqn (18), the EOS Eqn (14) and the control volume calculation completely define the P-V relation for an inflated airbag.

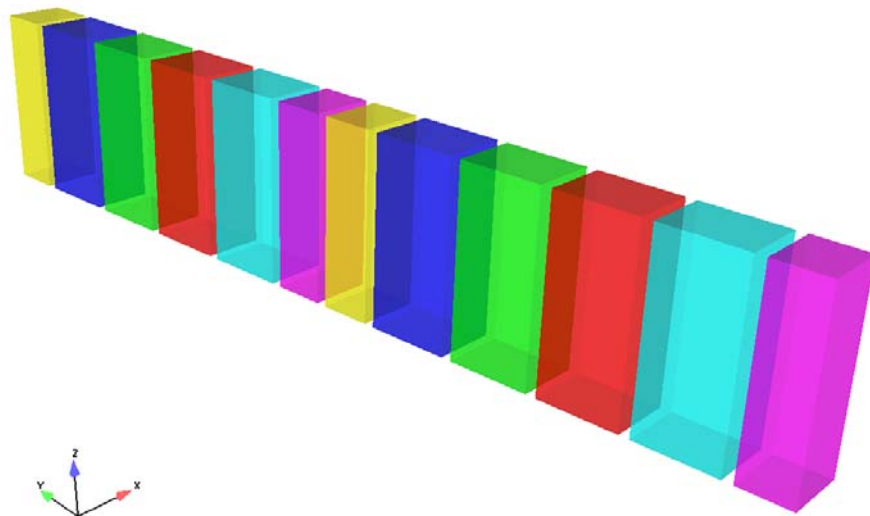


**Figure 10. Energy Absorbing Barrier Impact Analysis
Airbag 1 – 12 (12 control volume)**

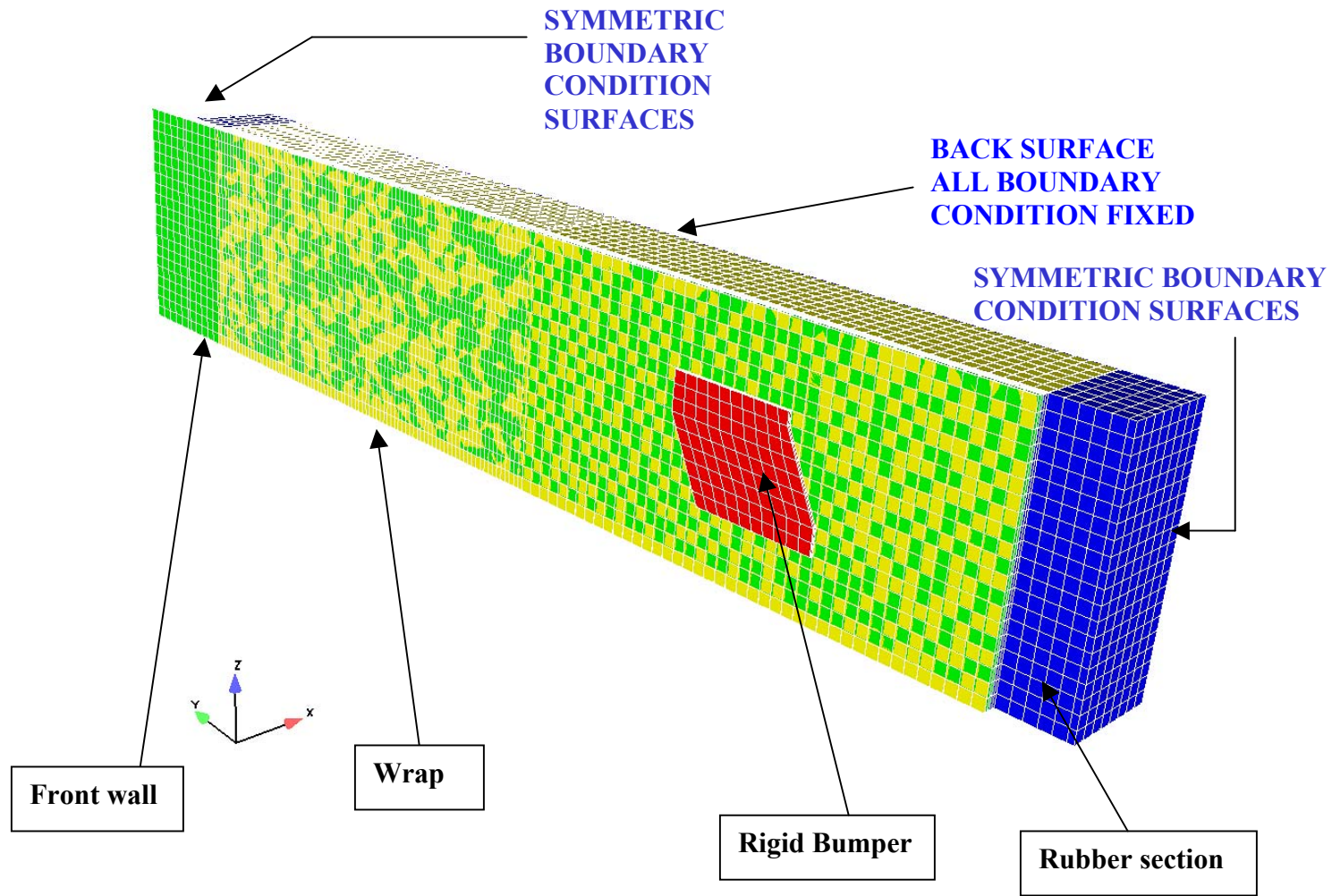


Figure 11. Energy Absorbing Barrier Impact Analysis
Wall Angle 0 Deg, Car hitting at 25.5° angle
Double Unit Block wrapped with 1/8" rubber skin

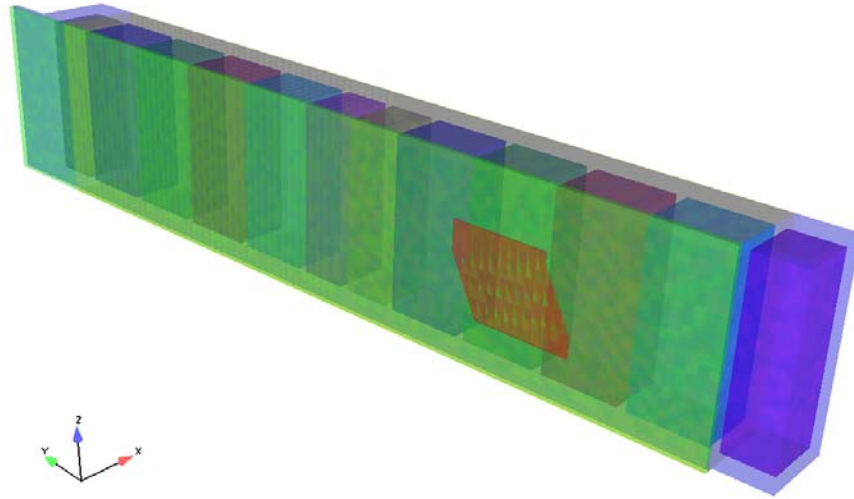


Figure 12. Energy Absorbing Barrier Impact Analysis, Full Model with airbags inside (Translucent view)

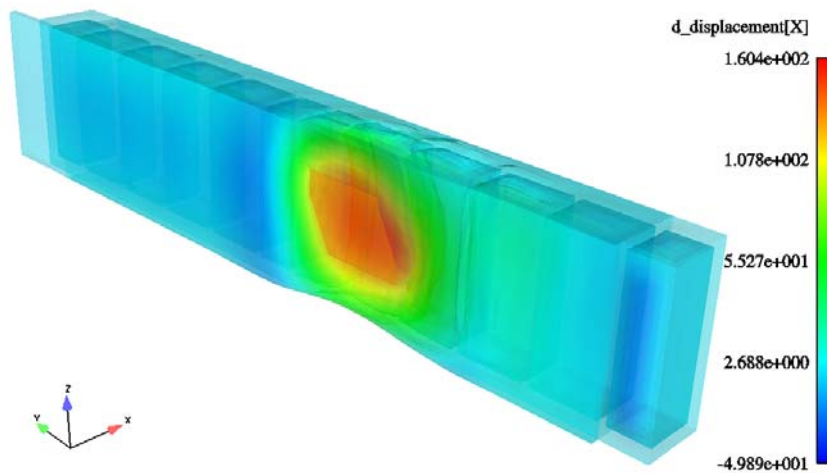


Figure 13. Energy Absorbing Barrier Impact Analysis, Full Model Axial deflection (mm)

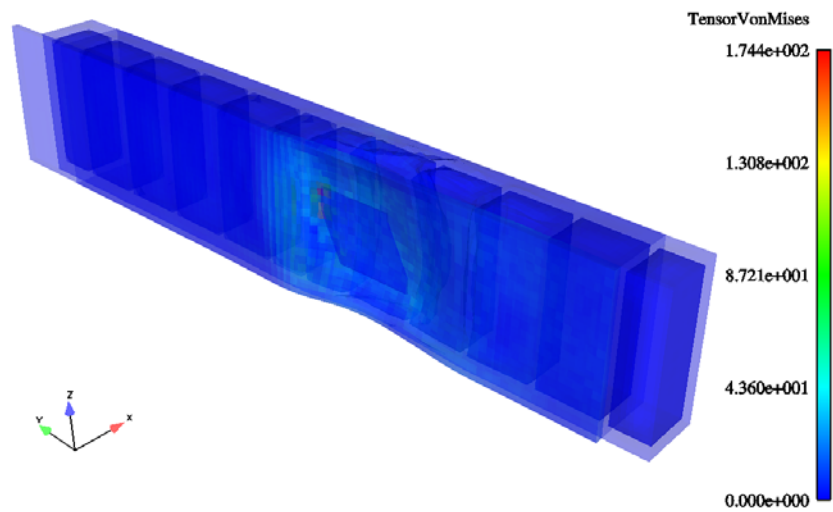


Figure 14. Energy Absorbing Barrier Impact Analysis, Full body VM Stress Plot (MPa)

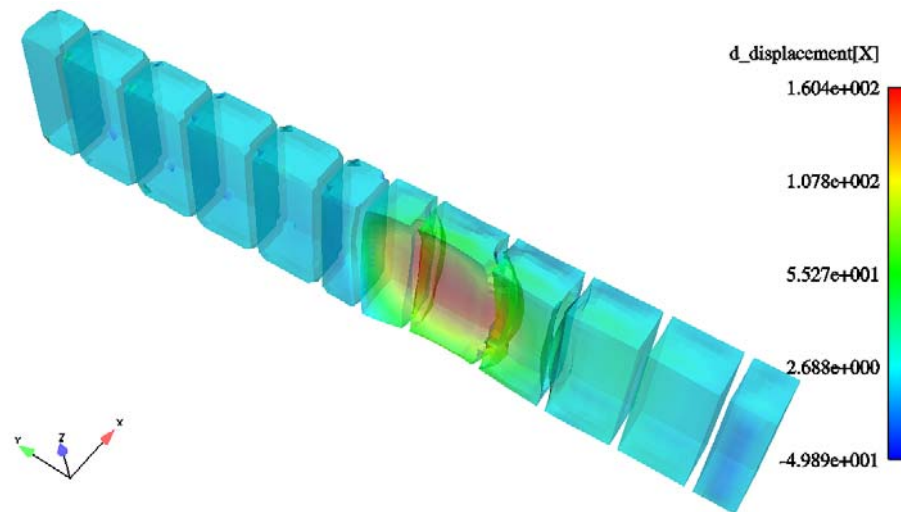


Figure 15. Energy Absorbing Barrier Impact Analysis Airbag Deformation Plot (mm), ISO view

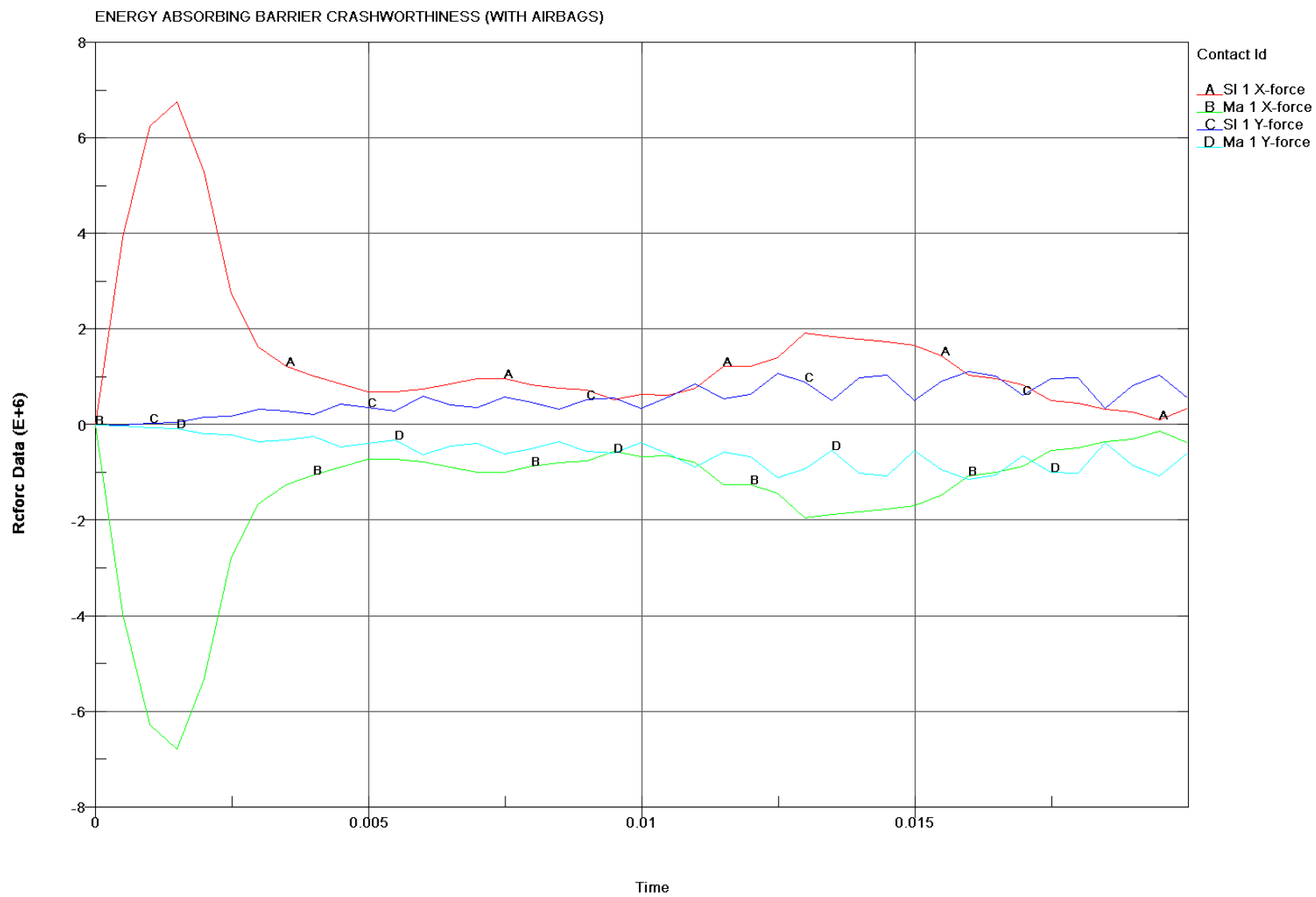


Figure 16. Reaction Force vs. Time

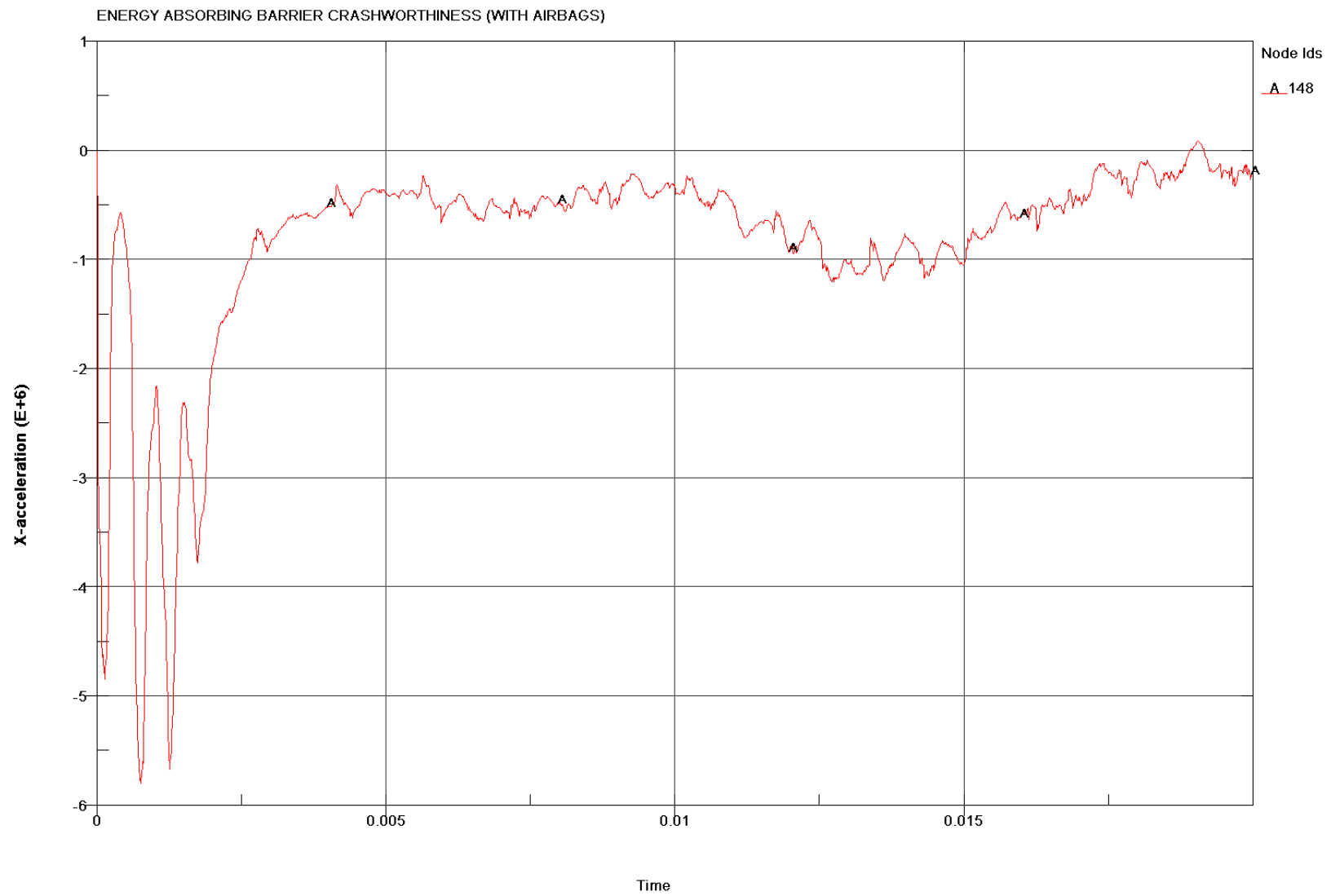


Figure 17. Unfiltered G load vs. Time

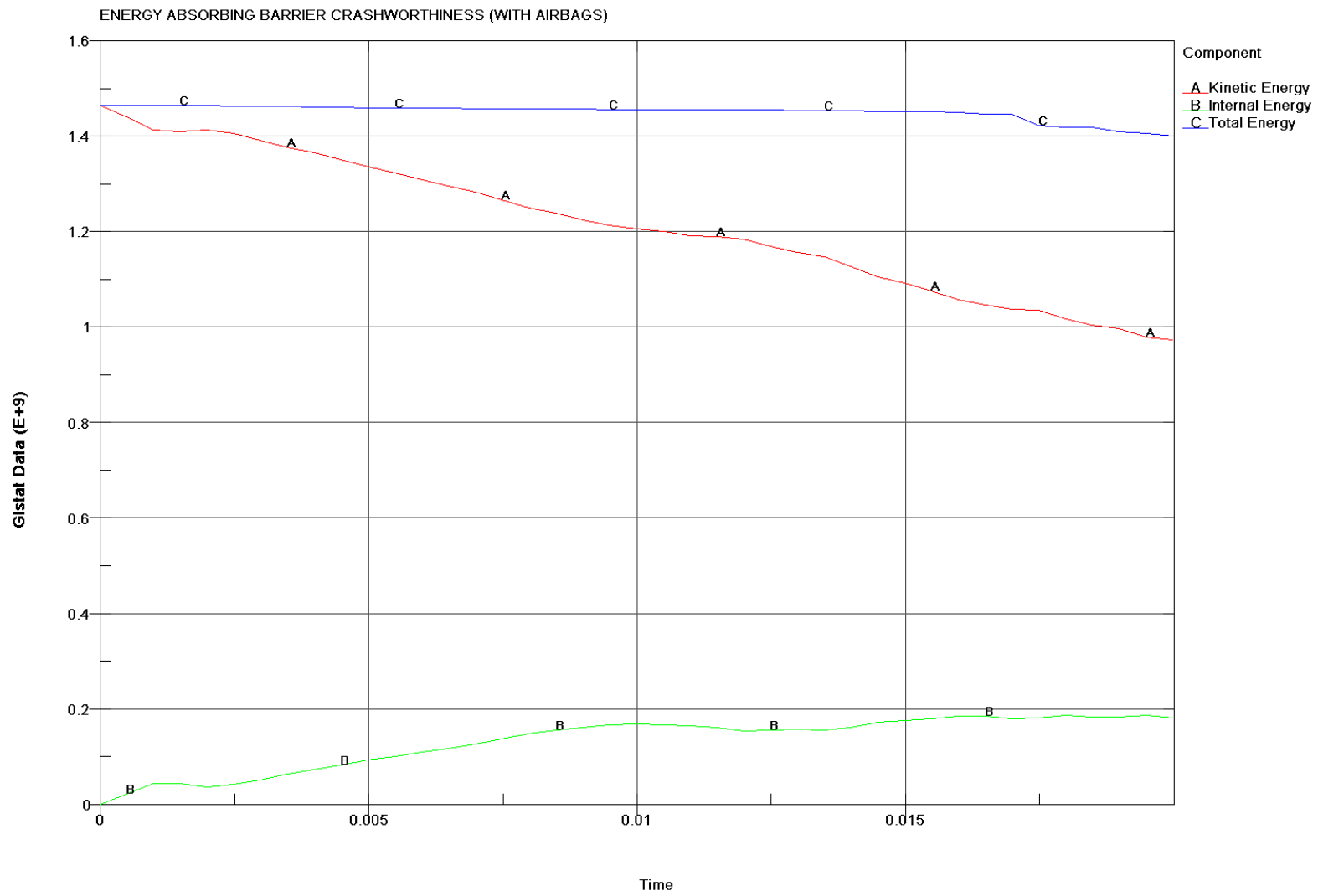


Figure 18. Global Energy vs. Time

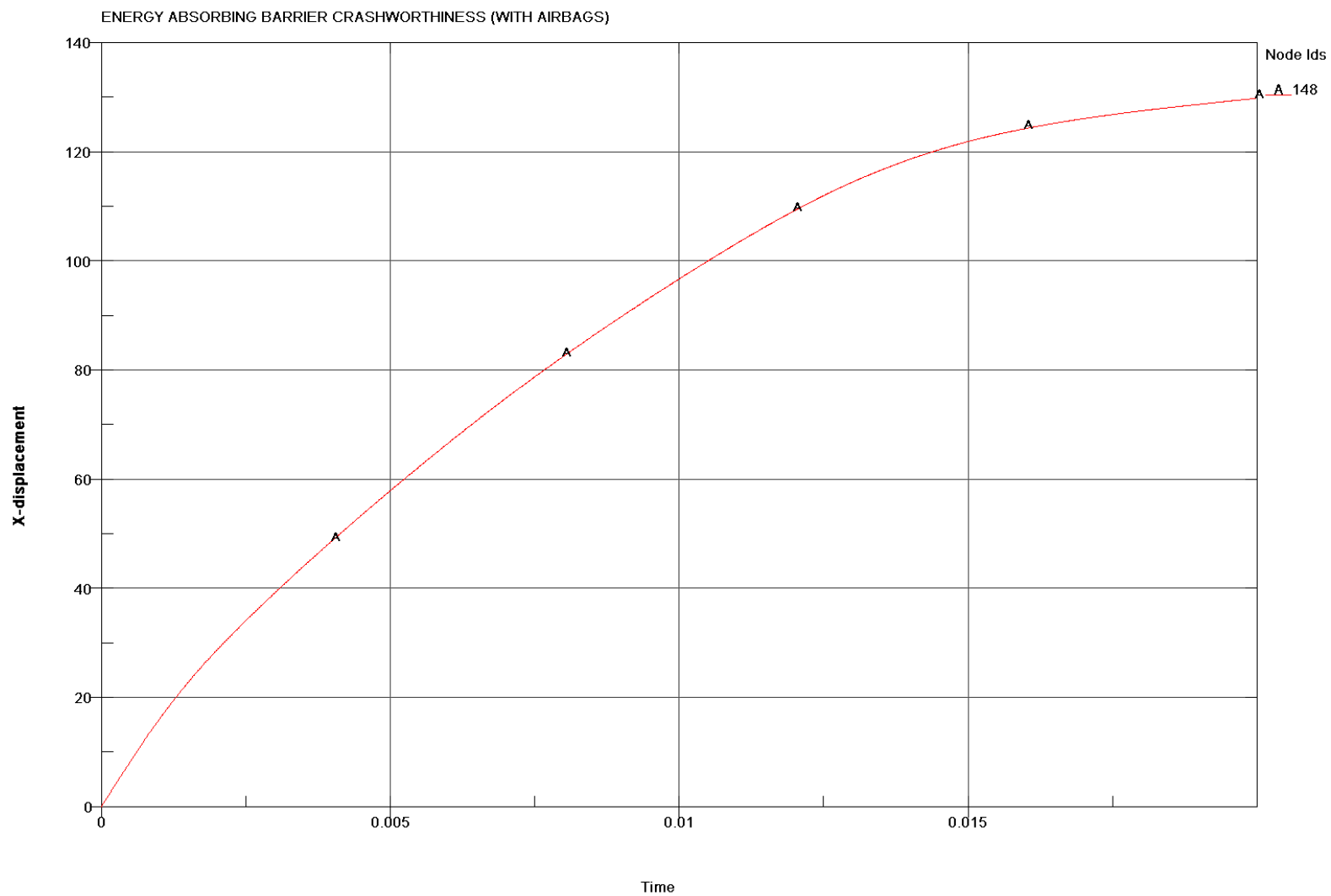
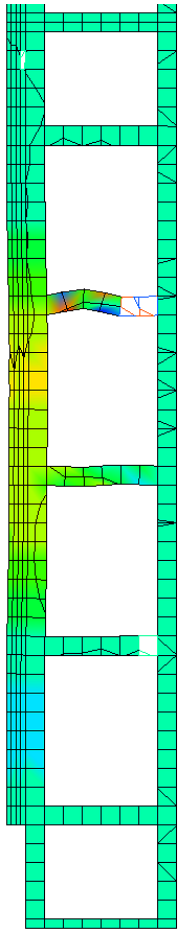
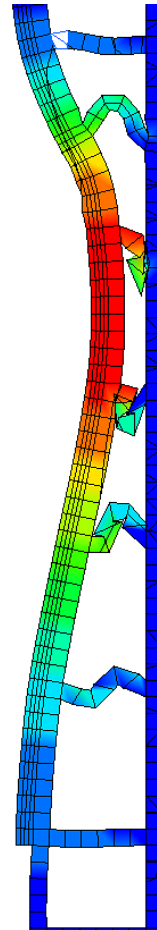


Figure 19. X Displacement vs. Time

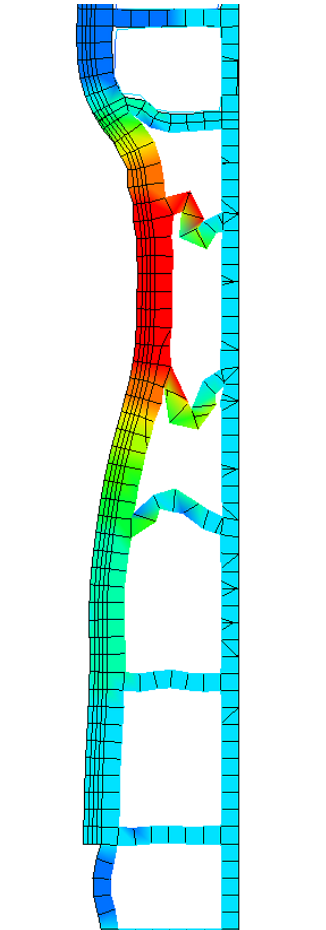
Figure 20: Concrete Barrier versus Airbag EAB, Impact Performance Comparison



**[a] CONCRETE BARRIER
SECTION VIEW @ 3 MS**



**[b] EAB (WITHOUT AIRBAG)
SECTION VIEW @ 20 MS**



**[c] EAB (WITH AIRBAG)
SECTION VIEW @ 20 MS**

COMPARISON WITH CONCRETE BARRIER AND EAB (W/O AIRBAG)

Concrete Material Property

$$\text{Density} = 2320 \text{ Kg/m}^3 = 2.32 \text{ E-9 T/ mm}^3 = 0.0838 \text{ lb/in}^3$$

$$E = 30 \text{ E9 N/m}^2 = 30 \text{ E3 N/ mm}^2 = 4.27\text{E7 psi, } \nu = 0.2$$

Table 2. Summary of 90 MPH impact results (with airbag)

| | DX (mm) | Impact Force (KN) | VMS (MPa) | | | Peak G Load (Axial, Unfiltered) |
|-----------------------|----------------|--------------------------|-------------------|--------------------|-------------|----------------------------------------|
| | | | | | | |
| Concrete | 13.39 | 45000 | 843 | | | 3300 |
| | | | | | | |
| | | | Front Wall | Rubber Wall | Wrap | |
| | | | | | | |
| Without Airbag | 244 | 3800 | 131 | 41 | 55 | 480 |
| | | | | | | |
| With Airbag | 162 | 6780 | 174 | 35 | 55 | 580 |
| | | | | | | |
| UTS | | | 47 | 19 | 19 | |

DISCUSSION BASED ON LSDYNA-3D ANALYSIS

Figure 10 shows the 12 airbag control volumes used in the simulation. Figures 12-15 show the axial displacement and VMS plots. Figures 16 – 19 show the time dependent plots of reaction force, unfiltered G load, energy and displacement. Figure 20 shows the comparative deformed plots of concrete barrier versus Energy Absorbing Barrier with and without airbag effect. It is clear that the concrete barrier absorbs very little energy and deforms very little compared to the flexible EAB. The peak G load is almost 8X that of the flexible EAB, which translates into extreme damage for the vehicle and extreme injury for the passengers. Nonlinear material property (stress-strain curves) has not been incorporated in the model. The peak VM stress values are higher than the UTS indicating failure of the EAB; however, the linear elastic material properties tend to overestimate the stresses during plastic deformation. The inclusion of nonlinear material properties would lower the VM stresses in the EAB components.

CONCLUSIONS BASED ON LSDYNA-3D ANALYSIS

The following conclusions are based on LSDYNA-3D nonlinear dynamic finite element simulation for airbag EAB.

- Finite Element Models of an airbag EAB for vehicular impact is developed to perform racecar crash simulation using LSDYNA-3D simulation. These Finite Element models are used to predict the magnitude of impact forces, G loading, Deformation, Stresses as a function of racecar velocity and the angle of impact.
- Quasi Static FEA over predicted deformation compared to LSDYNA-3D.
- The peak axial deformation for the EAB with the airbag is 30% lower than the EAB without the airbag effect, while the G loading is almost identical.
- The stresses for the EAB with the airbag are higher compared to those from the EAB without the airbag due to increased stiffness (the airbag effect).
- Nonlinear material property (stress-strain curves) has not been incorporated. The peak VM stress values are higher than UTS indicating failure of the EAB. Since linear elastic material properties tend to overestimate the stresses during plastic deformation, the inclusion of nonlinear material properties would lower the VM stresses.
- The effect of cutouts on the airbag surface is studied; however, no appreciable change in displacement or stress is noticed for the main parts for small changes in the cutout diameter. This issue needs to be further investigated.
- Worst-case scenario of impact is studied using a rigid bumper.
- An actual racecar would be more flexible and the peak G load and wall deformation would be lower than this research exhibits.

RECOMMENDATIONS BASED ON LSDYNA-3D ANALYSIS

The following discussion is based on LSDYNA-3D nonlinear dynamic finite element simulation for airbag EAB.

- Non-linear material properties should be included in the LSDYNA-3D simulation.
- Racecar crash simulations should be performed at 153 MPH peak velocity.
- The effect of cutouts on airbag surfaces should be further explored.
- An actual racecar impact could be studied for peak G load and wall deformation.

ACKNOWLEDGEMENTS

This work has been supported by the Center for Advanced Materials and Smart Structures (CAMSS) and Safety Systems Inc (SSI).

REFERENCES

- 1] Bligh, Roger, *ASSESSMENT OF NCHRP REPORT 350 TEST CONDITIONS*, Texas Transportation Researcher Magazine, Texas Transportation Institute.
- 2] Consolazio, Gary R., Chung, Jae H., Gurley, Kurtis R., *Development of a Low Profile Work Zone Barrier Using Impact Finite Element Simulation*, Transportation Research Board, Submitted for review
- 3] Consolazio, Gary R., Chung, Jae H., Gurley, Kurtis R., *Impact simulation and full scale crash testing of a low profile concrete work zone barrier*, J Computers and Structures, 2003
- 4] Botkin, Mark, E., Johnson, Nancy, L., Zywick, Ed., Simunovic, Srdan, *Crashworthiness Simulation of Composite Automotive Structures*, 13th Annual Engineering Society of Detroit Advanced Composites Technology Conference and Exposition, Detroit, Michigan, September 28-29, 1998
- 5] Reid, John D., Faller, Ronald K., Holloway, Jim C., Rohde, John R., Sicking, Dean L., *A New Energy-Absorbing High-Speed Safety Barrier*, TRB 2003 Annual Meeting
- 6] Jiang, T, Grzebieta, R. H. and Zhao, X. L., *Predicting impact loads of a car crashing into a concrete roadside safety barrier*, International Journal of Crashworthiness, Volume 9, Number 1, pp 45 – 63.
- 7] Karma, Yonten, Manzari, Majid T., Eskandarian, Azim, Marzougui, Dhafer, *AN EVALUATION OF CONSTITUTIVE MODELS OF CONCRETE IN LS-DYNA FINITE ELEMENT CODE*, 15th ASCE Engineering Mechanics Conference, June 2-5, 2002, Columbia University, New York, NY
- 8] Kelkar, A. D., and Schulze, M., J., *Simulation of the Ford Taurus Frontal Offset Impact into the EEVC Fixed Deformable Barrier*, NHTSA Final Report, September 24, 1996.
- 9] Kirkpatrick, Steven W., MacNeill, Robert, and Bocchieri, Robert T., *Development of an LS-DYNA Occupant Model for use in Crash Analyses of Roadside Safety Features*, ARASVO, August 2002.
- 10] Mackerle, Jaroslav., *Finite Element Crash Simulations and Impact-Induced Injuries: An Addendum. A Bibliography (1998-2002)*, The Shock and Vibration Digest, Vol. 35, No. 4, 273-280 (2003)

11] Ray, M. H., *Repeatability of Full-Scale Tests and Criteria for Validating Simulation Results*, Transportation Research Record No. 1528, Transportation Research Board, National Academy Press, Washington, D.C., 1996.

12] Wekezer, J.W., and Cichocki, K., *Numerical analysis and experimental verification of vehicle trajectories*, J. Phys. IV France 110 (2003) 377